BMC Genomics

BioMed Central

Research article

Open Access

Genome-wide mapping of ORC and Mcm2p binding sites on tiling arrays and identification of essential ARS consensus sequences in *S. cerevisiae*

Weihong Xu†, Jennifer G Aparicio†, Oscar M Aparicio* and Simon Tavaré*

Address: Molecular and Computational Biology Program, University of Southern California, Los Angeles, CA, USA

Email: Weihong Xu - weihongx@usc.edu; Jennifer G Aparicio - japarici@usc.edu; Oscar M Aparicio* - oaparici@usc.edu; Simon Tavaré* - stavare@usc.edu

* Corresponding authors †Equal contributors

Published: 26 October 2006

BMC Genomics 2006, **7**:276 doi:10.1186/1471-2164-7-276

Received: 18 May 2006
Accepted: 26 October 2006

This article is available from: http://www.biomedcentral.com/1471-2164/7/276

Abstract

Background: Eukaryotic replication origins exhibit different initiation efficiencies and activation times within S-phase. Although local chromatin structure and function influences origin activity, the exact mechanisms remain poorly understood. A key to understanding the exact features of chromatin that impinge on replication origin function is to define the precise locations of the DNA sequences that control origin function. In *S. cerevisiae*, Autonomously Replicating Sequences (ARSs) contain a consensus sequence (ACS) that binds the Origin Recognition Complex (ORC) and is essential for origin function. However, an ACS is not sufficient for origin function and the majority of ACS matches do not function as ORC binding sites, complicating the specific identification of these sites.

Results: To identify essential origin sequences genome-wide, we utilized a tiled oligonucleotide array (NimbleGen) to map the ORC and Mcm2p binding sites at high resolution. These binding sites define a set of potential Autonomously Replicating Sequences (ARSs), which we term nimARSs. The nimARS set comprises 529 ORC and/or Mcm2p binding sites, which includes 95% of known ARSs, and experimental verification demonstrates that 94% are functional. The resolution of the analysis facilitated identification of potential ACSs (nimACSs) within 370 nimARSs. Cross-validation shows that the nimACS predictions include 58% of known ACSs, and experimental verification indicates that 82% are essential for ARS activity.

Conclusion: These findings provide the most comprehensive, accurate, and detailed mapping of ORC binding sites to date, adding to the emerging picture of the chromatin organization of the budding yeast genome.

Background

Eukaryotic chromosomal DNA replication initiates from numerous loci, termed replication origins, distributed along each chromosome. The selection of chromosomal sites that will function as origins begins with the binding to DNA of the Origin Recognition Complex (ORC) [1,2]. During late M and early G1 phases, ORC, together with Cdc6 and Cdt1, directs the loading onto origin DNA of MCM complexes to assemble pre-replicative complexes (pre-RCs). Upon S-phase entry, activation of pre-RCs

leads to DNA unwinding and the assembly of replisomes that carry out DNA synthesis [3,4]. Origins differ in their timing of activation during S-phase and their frequency of activation (maximum once per cell cycle). A clear understanding of factors that influence the efficiency and timing of initiation is lacking, although histone modification, nucleosome positioning, and transcription have been implicated [5-11]. Chromatin structure also appears to influence the selection of ORC binding sites [1,12,13].

In most eukaryotic cells, specific sequences do not appear to be required for ORC binding [13-15]. For example, in fission yeast, almost any highly A/T-rich sequence of sufficient length (~1 kb) can function as a replication origin. In *Xenopus* egg extracts and *Drosophila* embryos, apparently random, closely spaced DNA sequences serve as replication origins to facilitate rapid cell (nuclear) division cycles. During embryogenesis, the number of sites used as origins decreases with the onset of transcription. This correlation suggests that the establishment of chromatin domains related to transcription limits the number of ORC binding sites in the chromatin. In mammalian cells, transfection of almost any DNA fragment of sufficient length can support replication, suggesting that ORC binding is generally stochastic but requires the presence of an accessible region in the chromatin. Furthermore, the activity of certain sequences as replication origins in mammalian cells correlates with local differences in gene expression in different cell types or lineages [16-19].

Saccharomyces cerevisiae differs somewhat in that specific DNA loci that function as replication origins (termed Autonomously Replicating Sequences or ARSs) contain a consensus sequence (ARS Consensus Sequence or ACS) that is essential for ORC binding and origin function [1,20,21]. However, an ACS alone is not sufficient for origin function and this sequence is much more abundant than the number of ORC binding sites or functional replication origins [20,22]. In addition to an ACS, ARSs contain at least one A/T-rich region of DNA thought to act as a DNA unwinding element. Although an unwinding element is important for origin function, it is not required for ORC binding [23]. Thus, despite its sequence preference, it remains unclear exactly how ORC binding sites are selected from the many potential sequences; however, local chromatin structures and activities are probably important factors. Indeed, the great majority of origins locate to intergenic regions [24]. While this and other studies suggest active transcription and origin function are antagonistic [25,26], the effect of transcription factors on local chromatin can also be important. Detailed analysis of ARS1 suggests that factors that position nucleosomes surrounding origins (including ORC itself) influence origin initiation efficiency [5,27-29]. Additional information on the chromatin organization in relation to ORC at a variety of origins exhibiting different characteristics (e.g. timing, efficiency, chromosomal location) should yield valuable insights into the mechanisms that regulate origin function. A precise mapping of ORC binding sites throughout the genome is an important step in this direction.

The advent of DNA microarrays has enabled the genome-wide analysis of DNA replication dynamics and identification of replication origins in a number of eukaryotic organisms [30,31]. In *S. cerevisiae*, various approaches have been fruitful. Some studies have directly analyzed replication timing by monitoring the time at which specific DNA sequences double in copy number or incorporate a chemically distinct precursor (e.g. density-substitution) [32,33]. A very recent study mapped the presence of single-stranded DNA during replication, which is expected to identify sites undergoing DNA synthesis [34]. These types of studies have provided valuable data on the overall dynamics of genome duplication. These studies also identified the positions of ~300 active replication origins, typically to within several kilobases (4–10 kb).

An alternative approach to identifying replication origins used genome-wide location analysis to determine the positions of ORC and MCM proteins [24]. This study identified 429 sites predicted to have ARS function with a resolution of ~1 kb. This level of resolution facilitated experimental validation of the data set, demonstrating 79% positive predictive value (PPV, defined as the percentage of true sites among all called sites). Because this particular study analyzed the position of static protein complexes, it provided a more precise mapping than the timing-based studies, but did not by itself characterize the activity of the predicted sites. Thus, the replication dynamics and protein location analyses provide complementary information to help create an accurate description of genome duplication. These studies did not attempt to identify the exact DNA sequences (ACSs) bound by ORC, which are essential for origin function. However, one study has identified potential ACS using a purely sequence-based search algorithm (Oriscan) [22]. Among the top 350 Oriscan sites (which is similar to the total number of origins predicted or inferred by other studies), 56% matched known ARS or proARS sequences.

To provide a more accurate and complete map of essential origin sequences that bind ORC, we performed genome-wide location analysis of ORC and Mcm2p with a high-density, tiled oligonucleotide microarray. The 529 ORC and/or Mcm2p binding sites revealed potential ARSs with high accuracy. The resolution of this analysis allowed for precise localization of hundreds of functional ACSs,

which serve as ORC binding sites, throughout the genome.

Results

Genome-wide identification of ORC and Mcm2p binding sites

Previously, we used genome-wide location analysis to map chromosomal binding sites of ORC and MCM proteins to about 1 kb resolution using DNA microarrays [21,24]. These microarrays contained about 12,000 cDNA probes, typically one for each open reading frame (ORF) and one for each intergenic region of the *S. cerevisiae* genome, with an average probe size of 618 bp. To map ORC and MCM binding sites with greater precision and facilitate the identification of ACSs within the identified binding regions, we performed genome-wide location analysis of ORC and Mcm2p using tiled oligonucleotide microarrays (NimbleGen) containing one 50mer oligonucleotide to represent each 80 bp segment of the genome, in triplicate. DNA enriched for ORC and Mcm2p binding sites was isolated by chromatin immunoprecipitation (ChIP) of ORC from M-phase cells and Mcm2p from G1-phase cells, respectively. Immunoprecipitated and total genomic DNA from each sample was differentially labeled and co-hybridized to the arrays.

Data were analyzed as outlined in Figure 1A (and see Methods). Briefly, a two-state Hidden Markov Model (HMM) with a mixture of Gaussian outputs was used to model the data (Figure 1B and see Additional file 1). This analysis identified 400 ORC-enriched regions and 634 MCM2-enriched regions. The ORC and MCM2 enriched regions intersect at 353 sites. Because the ORC and MCM2 intersecting regions generally do not overlap exactly, the union is used in defining a single site, resulting in 349 discrete (non-overlapping) regions that we refer to as ORC-MCM2 sites. The HMM-called regions, a total of 677 discrete sites, are divided into three groups: 47 ORC-only sites, 281 MCM2-only sites and 349 ORC-MCM2 sites (see Additional files 2, 3, and 4, respectively).

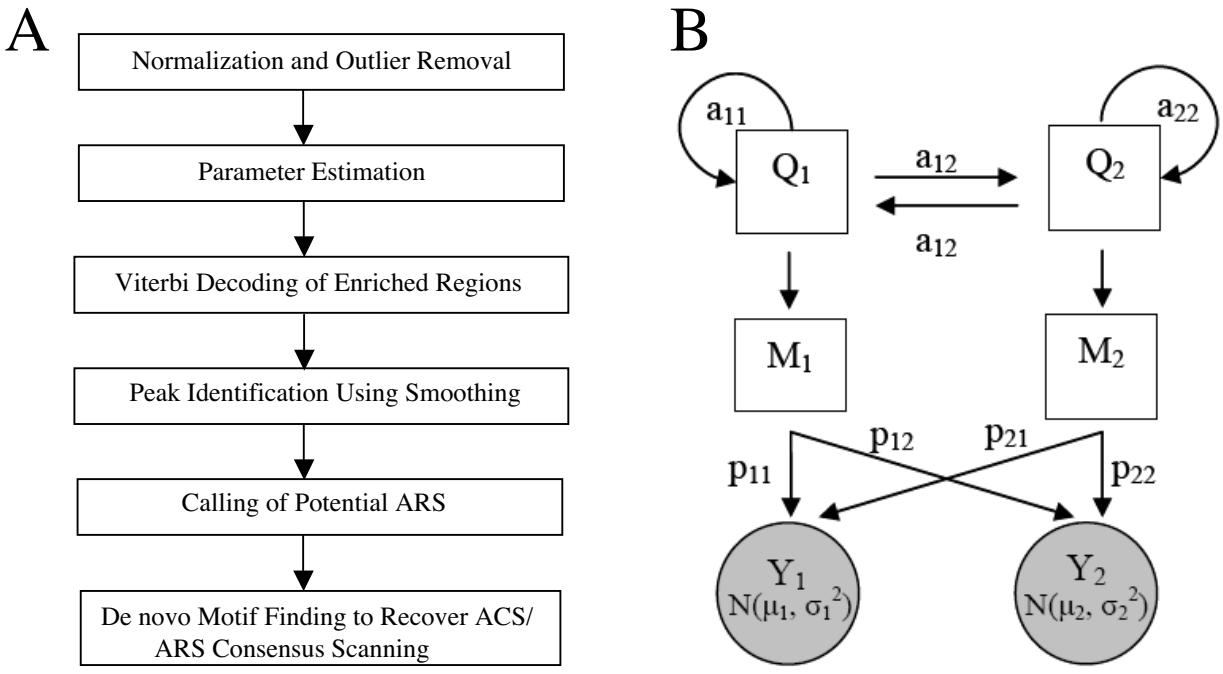

Figure 1
Analysis of ORC and Mcm2p whole genome localization experiments using a tiled oligonucleotide array. **A**. Strategy. **B.** The Hidden Markov Model with Mixture of Gaussian output. Round shapes represent continuous variables and square shapes represent discrete variables. Gray refers to observed variables.

On these tiled oligonucleotide arrays, the immunoprecipitated target DNA (average shear size of ~1 kb) is expected to identify numerous probes for each binding site, with the probes' standardized log2 signal intensities (Z) forming a peak centered very close to the actual protein binding site. To locate the peak probe more accurately, the Z-values were smoothed using a moving average (see Methods). Within each HMM-called region, peaks of ORC and/or MCM2 signal were identified based on a continuous increase of the smoothed Z values (sZ) for at least five probes followed by a continuous decrease of sZ for at least five probes. A corresponding peak strength was calculated as the average Z value (avgZ) (see Additional files 2, 3 and 4).

ARS prediction

We sought criteria to evaluate the merit of the three classes of binding sites for ARS prediction. The ORC-MCM2 class is anticipated to have the strongest predictive value because two different pre-RC proteins co-localize at these sites. Thus, we compared characteristics of the ORC-only and MCM2-only sites to the ORC-MCM2 sites. Among experimentally verified ARS sites, 95% are contained in the HMM-called data set (see Additional file 5); of these, 77% are defined by ORC-MCM2 sites, 23% by MCM2-only sites, and none by ORC-only sites. These results suggest that Mcm2p binding is a more sensitive predictor of ARS location than ORC binding.

Examination of peak strength shows that true ARSs are associated with robust signals. For the 89 known ARSs identified in this analysis, 95% of the MCM2 peaks and 92% of the ORC peaks had avgZ ≥ 2.75. Comparison of signal strength between the three classes of sites shows that, on average, peaks of ORC-only sites are significantly weaker than peaks of MCM2-only sites as well as peaks of ORC or MCM2 in ORC-MCM2 sites (rank sum test p-value < 0.001 for all cases). Furthermore, peaks of MCM2-only sites are on average significantly weaker than peaks of ORC or MCM2 in ORC-MCM2 sites (rank sum test p-value < 0.001) (Figure 2). Combined with the proportions of known ARSs associated with each of these classes, these findings suggest that ORC-only sites have the lowest, ORC-MCM2 sites the strongest, and MCM2-only sites an intermediate predictive value.

A *bona fide* ARS is anticipated to contain an ACS that serves as the ORC binding site. An objective search for a common motif in each group of binding sites using *de novo* motif finding recovered the ACS motif from the ORC-MCM2 sites (Figure 3). In fact, the recovered motif is very similar to the extended ACS (EACS) described by Theis and Newlon [21], and also 89% similar to the motif generated by alignment of 31 previously identified, functional ACSs (see Additional file 12). For the MCM2-only group, a motif that is 70% similar to the EACS is recovered. No significant motif is recovered from the ORC-only sites (Figure 3). (See Methods for a description of the calculation of inter-motif similarity.) These results further support the idea that ORC-MCM2 sites are accurate predictors of origins whereas ORC-only sites appear to be poor predictors. The MCM2-only group probably contains a greater proportion of non-ARS sequences than the ORC-MCM2 group, complicating identification of the ACS motif in this group.

As ORC-MCM2 sites have a stronger average MCM2 peak signal than the average peak signal of the MCM2-only class, a threshold peak signal (avgZ ≥ 2.75) was established to select MCM2-only and ORC-only regions with a high probability of ARS activity. These were included in the set of potential ARSs called "nimARS". In total, 529 nimARS sites are defined, including 349 ORC-MCM2 sites, 178 MCM2-only sites, and two ORC-only sites (see Additional file 6). This data set includes 95% of experimentally confirmed ARSs (thus the sensitivity is 95%; sensitivity is defined as the percentage of sites that are called among all true sites in the genome). The chromosomal distribution of these sites is shown in Figure 4.

Validation of ARS predictions and comparison with previous studies

Our analysis predicted 52 nimARS loci on chromosomes I and II. We tested the ARS function of 46 of these loci (five had been previously confirmed and one resisted analysis), and found that all but two have ARS activity (Table 1 and see Additional file 10). We also tested eight sites on chromosome X that were not predicted in the previous pro-ARS data set [24]. ARS activity was confirmed for six of these sites (3 strong, 2 weak and 1 very weak activity), one lacked activity, and one resisted analysis. On chromosomes III and VI, for which ARS activity has been comprehensively tested [35-37], the nimARS set predicts five new sites. Experimental analysis of these sites showed weak ARS activity for three sites, and two lacked activity (Table 1 and see Additional file 10). Comparing the cumulative experimental results from chromosomes I, II, III, VI, and X shows 94% PPV of the nimARS predictions (Table 1 and see Additional file 10) [24,35-37].

Comparison of our data with previous array-based origin predictions demonstrates considerable overlap. A Venn diagram shows the intersection of four data sets, proARS [24], timeARS [32], ssARS [34] and the current nimARS (Figures 5A and 5B). The criterion used to define corresponding sites is overlap between the defined regions. For the 332 timeARSs the region is defined as the 5 kb flanking each side of the peak. Of these timeARS regions, 231 (70%) intersect with 261 (49%) nimARS regions. For the 364 ssARS, the region is defined as the 4 kb flanking each

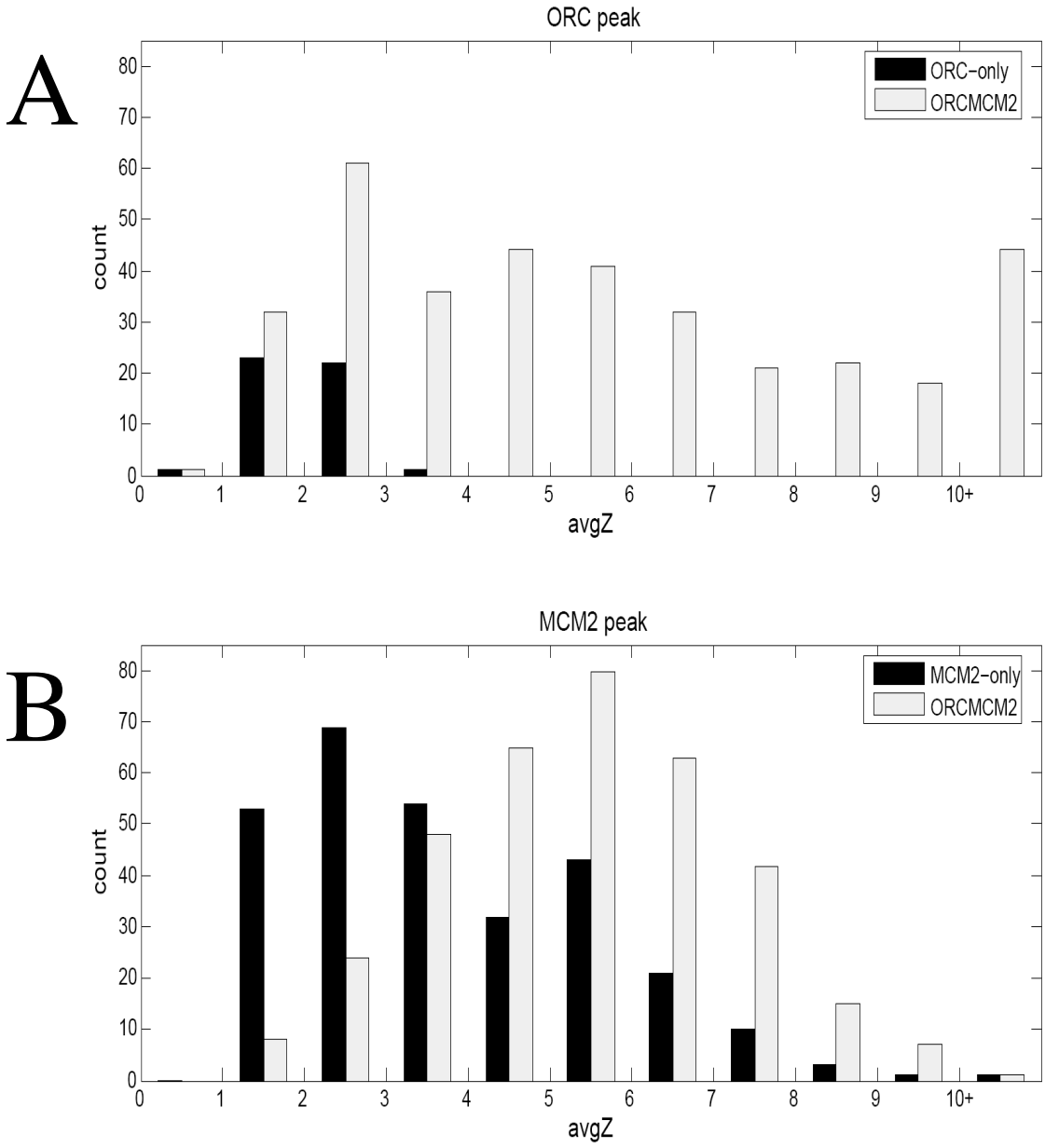

Figure 2
Peak strength in the three classes of binding sites. **A**. Comparison of ORC peak strength within ORC-only sites and ORC-MCM2 sites. **B**. Comparison of MCM2 peak strength within MCM2-only and ORC-MCM2 sites.

Data*	Number of Occurrences	Average Number of Occurrences	p-value	logo
Known ACS (31)	31	1	NA	
ORC-MCM2 (349)	410	1.18	7.3×10^{-142}	
MCM2 (281)	287	1.02	1.3×10^{-8}	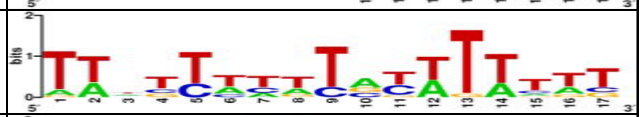
ORC (47)	51	1.09	9.0×10^{-5}	

Figure 3

De novo motif finding within ORC-MCM2, MCM2-only and ORC-only sites. *Numbers in parentheses refer to the number of input sequences in each set. "Known ACS" denotes an alignment of 31 ACSs identified by mutation analysis and is provided for comparison. The sequence logo was generated using Weblogo [65].

side of the average position of ssDNA peaks at three time points. For this case, 301 (57%) nimARS regions intersect with 303 (83%) ssARS. The high overlap of nimARS with both timeARS and ssARS strongly suggests that nimARS includes the majority of active ARSs. Among the proARS sites, 342 (80%) overlap with 331 (63%) nimARS sites, numbers that closely correspond to the expected number of positives in the proARS data set (0.79 × 429 = 338). We tested 22 proARSs that do not overlap with a nimARS site and found that all 22 lack ARS activity (see Additional file 11). This finding underscores the greater accuracy of nimARS data. Also notable is the detection of ARS304 (MCM2-32), ARS319 (ORCMCM2-41) and ARS604 (ORCMCM2-105), three known ARSs that are inactive as chromosomal origins and have not been previously detected using array methodologies [24,32-35,37]. In fact, testing of 26 additional sites not identified by any previous array studies shows that 80% (21 of 26) have ARS activity, although this activity is frequently weak (see Additional file 10). The identification of numerous new ARSs indicates that the current analysis has higher sensitivity than previous studies, and includes some sites that have marginal activity.

ORC and Mcm2p binding within nimARS regions

Use of tiled oligonucleotide arrays yielded high-resolution data for which certain characteristics of ORC and Mcm2p binding *in vivo* as analyzed by ChIP could be examined. The mean lengths of individually defined ORC and MCM2 regions within the set of ORC-MCM2 sites are not significantly different (signed rank test of equality has p-value = 0.89), suggesting that the ORC and MCM complexes associate with similar lengths of chromatin (Figure 6A). To assess the relative positions of ORC and Mcm2p, we compared the distance between the ORC and MCM2 peaks within the ORC-MCM2 sites (Figure 6B). The peak of the ORC or MCM2 signal within each binding site is anticipated to identify the oligonucleotide probe closest to the protein-binding site. Although there was a significant range to the data, the most common occurrence was co-localization of the ORC and MCM2 peaks to the same probe, which represents an 80 bp region. These data are consistent with ORC and MCM proteins occupying similar locations within ARS chromatin.

ACS identification

Peak identification within the HMM-called regions provides a high-resolution map of ORC (and Mcm2p) binding that is expected to correspond to the location of an ACS. For the 31 ACSs that have been experimentally verified, ORC peaks are found on average 236 bp (95% confidence interval is 0 – 474 bp) from the defined ACS while MCM2 peaks average 222 bp (95% confidence interval is 0 – 525 bp) (Figure 7). A signed rank test shows no signif-

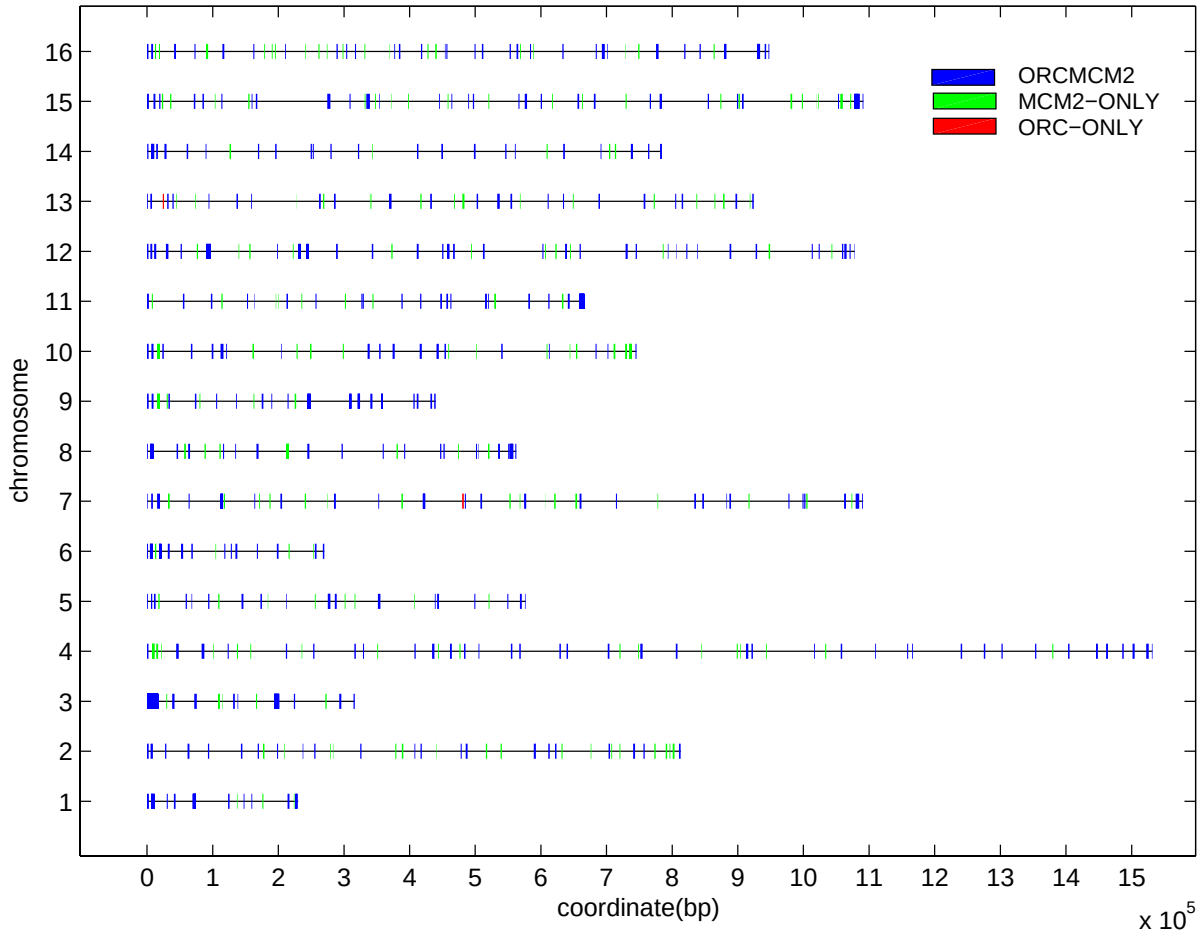

Figure 4
Distribution of nimARSs along the 16 *S. cerevisiae* chromosomes. Each horizontal line represents one chromosome. Blue bars represent nimARS sites identified by both ORC and MCM2; green bars represent nimARS sites identified by MCM2 only; and red bars represent nimARS sites identified by ORC only.

icant difference between the locations of the two distributions (p-value = 0.38). These distances are significantly shorter than the average shear size of the target DNA, suggesting that the shear size does not strictly limit the resolution on the tiling array due to presence of signal peaks in the data. The lack of a closer co-localization is at least partly due to the fact that probes corresponding to the exact ACS are frequently missing from the array due to the AT richness of these sequences (for examples, see Fig 7B).

The resolution of the nimARS data provides an opportunity to precisely define essential ACSs by narrowing a search to a relatively small region surrounding each nimARS data peak. A Positional Weight Matrix (PWM) generated from the 31 known ACSs yields a motif containing an EACS as well as three additional positions corresponding to the B1 element (of ARS1) (see Additional files 7 and 12). Interestingly, two of these three nucleotide positions had been previously mapped as sites of contact with ORC at ARS1 [38], suggesting this interaction is con-

Table 1: Summary of ARS testing results and known ARSs for nimARSs on five chromosomes.

Chromosome	*I*	*II*	*III*	*VI*	*X*	*Total*
Known ARS	2	3	13	13	22	53
ARS activity	11	33	0	3	6	53
No ARS activity	0	2	1	1	3	7
Untested	0	1	0	0	1	2
Total nimARS	13	39	14	17	32	115

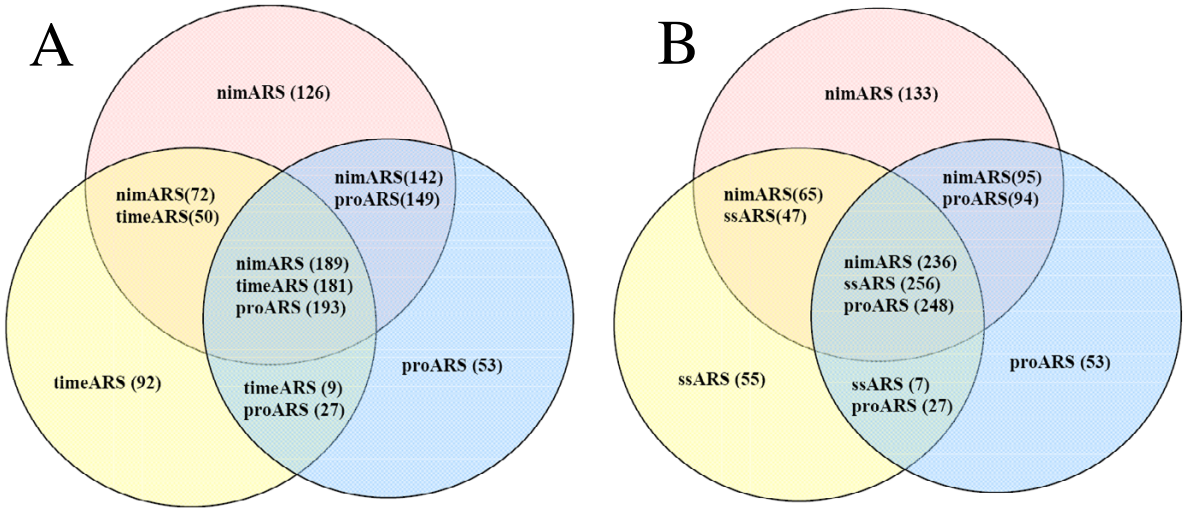

Figure 5
Venn diagrams showing overlap of data sets. **A.** nimARS, proARS [24] and timeARS [32]. **B.** nimARS, proARS and ssARS [34].

served. This EACS+B1 PWM was used to search a 1 kb window centered on each ORC and MCM2 peak. A 1 kb window was chosen because this roughly corresponds to the 95% confidence interval window for the distance of ORC and MCM peaks from known ACSs (see above). The EACS+B1 identified within the nimARS set are called nimACS (see Additional file 8). Using a p-value cutoff of 1.3×10^{-4}, we identified 506 nimACS in 370 nimARS (78% have single ACS, 22% have multiple ACSs, see Additional file 8). (In comparison, this method and p-value identifies 3271 EACS+B1 sites within the entire genome.) The percentage of nimARS with multiple nimACSs is close to the proportion of known ARSs with multiple functional ACSs (5/25). A three-fold cross-validation (see Methods) shows that the nimACS includes 58% of known ACSs (thus the sensitivity is 58%). The accuracy of the defined nimACSs was tested by mutating 17 ACSs predicted within 14 ARSs on chromosome X (see Additional file 9). For 11 of these ARSs, mutation of the single predicted ACS eliminated ARS function. For the remaining three ARSs in which two ACSs were predicted in each, one of the two sites was essential for ARS function while the other was dispensable. These results indicate a PPV of 82%.

Discussion

ARS identification in *S. cerevisiae* by genome-wide motif scanning has been hampered by the abundance of sequences with high similarity to the ACS, combined with the level of degeneracy of the ACS that supports function. Potential solutions to this problem include: (1) building larger motif models by including other concurrent motifs [39] or compositional information [22,40]; (2) assuming a specific motif distribution on chromosomes, e.g., a Hidden Markov Model [41,42]; and (3) narrowing down the regions to be searched. The first two methods rely on assumptions, which may introduce significant error. This study took the third approach, using a high-resolution array to map ORC and Mcm2p binding regions and confining the motif-search to this fraction (~5%) of the genome. A very recently published study took a fourth approach, analyzing phylogenetic conservation, in conjunction with motif searching and published microarray data to predict ACS locations [43].

We defined 529 nimARS loci throughout the *S. cerevisiae* genome that avidly bind ORC and/or Mcm2p. The vast majority of known ARSs (95%) are contained in the nimARS set and virtually all predicted sites exhibit ARS activity when tested (94%). Comparison to a recently determined set of chromosomally active replication origins (ssARS) shows that 83% are contained in the nimARS set [34]. Together, these analyses confirm the high accuracy of the nimARS data. The HMM analysis is capable of identifying even weak signals, while the target DNA identifies multiple probes on the tiled oligonucleotide array for each binding site, a redundancy that enhances accuracy. We further defined this data set by determining the signal peaks within the nimARS regions and constrained

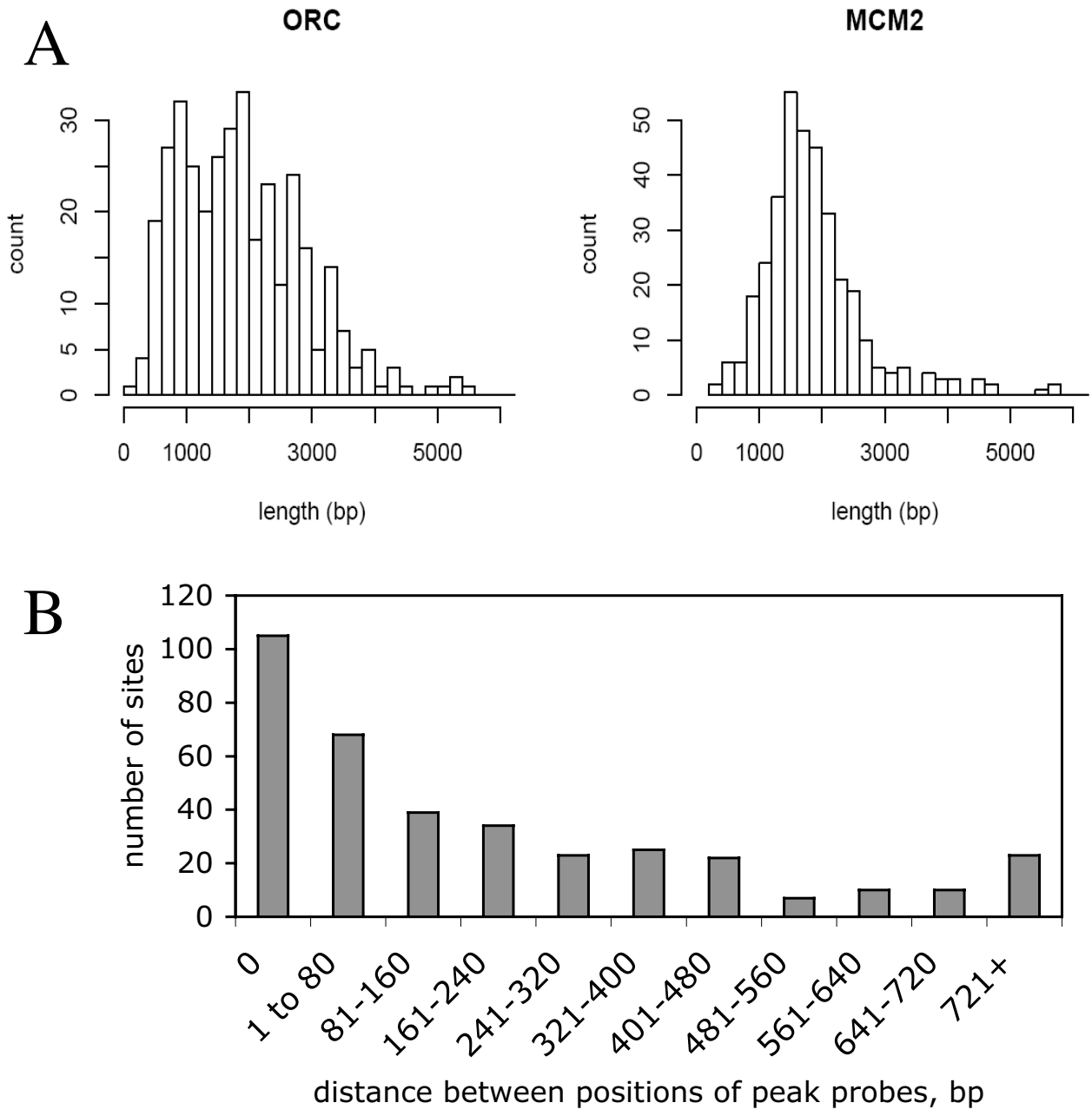

Figure 6
Comparison of ORC and MCM2 data within the set of ORC-MCM2 sites. **A.** Length of the ORC and MCM2 HMM-called regions is shown. **B.** Distance between the positions of probes that define ORC and MCM2 peaks in the ORC-MCM2 class of binding sites. Thus "0" means that the peaks identified are the same 50 bp probe and "721+" means that the peaks are more than 9 probes (spaced ~80 bp) apart.

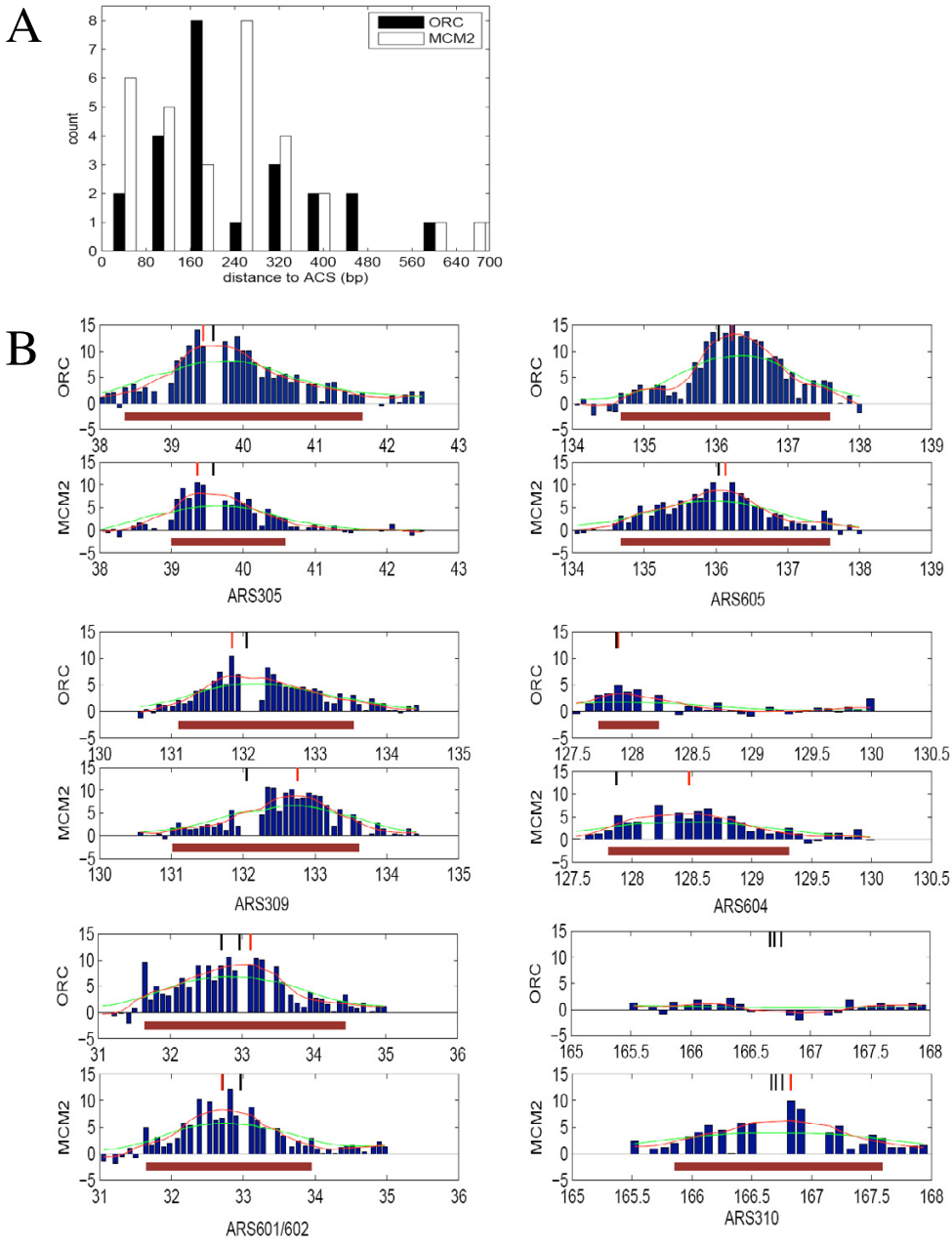

Figure 7
Known ACSs' locations relative to ORC and MCM2 peaks. **A.** Distance of known ACSs to closest ORC peak and MCM2 peak. **B.** Relative locations of ACS and ORC peak or MCM2 peak. The x-axis indicates the coordinates of probes on chromosomes in kilobases. The y-axis indicates signal strength by Z-value. The red tick attached to the top axis denotes the ORC or MCM2 peak and the black tick denotes the ACS location. The blue bars represent the Z-value at specified probe coordinates. The red and green lines indicate the smoothed Z-value (sZ) and average Z-value (avgZ) respectively. The horizontal red bar marks the regions called by HMM. For ARS305 and ARS605 both the ORC and MCM2 peaks are very close to the ACS location; for ARS309 and ARS604 the ORC peaks are located close to the ACS, but the MCM2 peaks are quite far due to shifted signal; ARS601/ARS602 and ARS310 have multiple proximate ACSs but do not confer multiple peaks in the data. Many ARSs show missing probes in the ACS region (15 out of 31 known ACSs have missing probes corresponding to the ACS).

the motif search to a 1 kb segment centered on each peak. Within 370 (70%) of the nimARS loci we identified at least one nimACS, with an overall PPV of 82%.

Approximately one-third of the predicted nimARSs are loci where only Mcm2p was detected. Of the nimARSs for which ARS activity has been demonstrated (in this or previous studies), 34% (52/152; see Additional files 5 and 10) are MCM2-only sites. This observation suggests that the majority of these sites will prove to possess ARS activity. Furthermore, ORC binding was not detected at 23% of known ARSs, while nimACSs, which predict ORC binding, are found at 103 of 178 of the MCM2-only sites. Finally, we have no evidence (such as a unique motif) suggesting that MCM2-only sites represent a distinct function of Mcm2p, which might be independent of ORC.

As ORC is bound to chromatin throughout the cell cycle in budding yeast and is required to "load" the MCM complex onto DNA, the detection of many MCM2-only sites suggests that ORC is present but recalcitrant to detection by ChIP, perhaps due to local chromatin differences. Indeed, we analyzed ORC binding in G2/M-arrested cells because pre-RC assembly is thought to occlude detection of ORC in G1-arrested cells [44]. However, we have recently found that ORC binding at some ARSs is more strongly detectable by ChIP during G1- or S-phase (JGA and OMA, unpublished). One possibility is that Cdc6 stabilizes binding of ORC to weaker sites during G1 to permit MCM loading [45,46]. This would explain the loading of Mcm2p in G1-phase at sites where ORC failed detection in G2/M, and is consistent with the idea that ORC occupancy and stability varies at different sites depending on local chromatin features or DNA sequence variation.

Whereas ORC detection by ChIP may be context- or cell cycle-dependent, Mcm2p seems to be more reliably detected. This may reflect differences in the way the ORC and MCM complexes interact with DNA. In contrast to models of ORC-DNA binding along the A rich strand of DNA [38], the MCM complex is thought to encircle one or both strands of DNA [47,48]. Such a topology might enhance cross-linking of MCM to chromatin or otherwise stabilize these complexes for immunoprecipitation. A greater stability of the MCM complex in pre-RCs is supported by *in vitro* data in which high salt extraction of pre-RCs removes ORC (and Cdc6) from DNA, but not the MCM complex [49-52].

Significantly more pre-RCs are formed than are normally utilized to replicate the genome. This work predicts about 500 pre-RCs are formed while other studies indicate that about 260–360 of these are primarily responsible for replicating the genome [32-34]. Some inefficient pre-RCs retain potential for activation but fail to initiate replication because replication forks emanating from efficient, nearby origins replicate through these sites, thereby eliminating their activation potential (presumably by dismantling the pre-RC) [53,54]. However, some sites at which ORC and/or Mcm2p can be identified exhibit relatively weak initiation potential. In some cases weak initiation is due to local chromatin, such as at the mating-type silencer ARSs, because these ARSs function efficiently when removed from their normal chromatin context [55]. However, some ARSs function poorly in the plasmid context, suggesting that sequence variation results in reduced ORC binding or inefficient DNA unwinding [56]. Sequence variation explains the failure to identify a robust ACS (EACS+B1) within about 30% of the nimARS. Further study will be required to determine how the sequence composition of the ACS and the surrounding sequences, as well as the presence of nearby motifs bound by other DNA binding proteins, contribute to the differential efficiency of ARSs (although specific cases, such as the silencer-associated with ARSs, have been identified [9,57,58]).

The molecular evolution of sequence and activity among different ORC binding sites (and related sequences) occurs under different selective pressures than that of individual genes or unique sequences with defined functions, as indicated by lower levels of phylogenetic conservation of yeast origins compared to genes [43]. This is because most individual ORC binding sites likely contribute little or nothing to the organism's fitness. The main requirement is that a sufficient number of efficient origins be distributed along each chromosome to ensure rapid genome duplication. Hence, sequence changes that increase the origin efficiency of one ORC binding site may reduce selective pressure on ORC binding sites on the same chromosome (especially nearby), resulting in weaker binding sites or even sites with specialized function such as the silencers. Origin sequence evolution also may derive from selective pressures on local gene functions if these are influenced by the presence of ORC. Nevertheless, the presence of excess ORC binding sites can help ensure efficient genome duplication in case the normal origin initiation program is disrupted [59], and hence, the ability of ORC to bind sequence variants is functionally significant. The ability of ORC to bind varied DNA sequences appears to be particularly important in higher organisms where ORC binding appears to conform to differential chromatin contexts related to developmentally regulated gene expression.

Conclusion

A central goal of current research in genomics is a precise and comprehensive mapping of all the protein-protein and protein-DNA associations that comprise the chromatin. Sequence-specific DNA-binding proteins such as ORC

are thought to play an important role in establishing the local chromatin architecture by influencing the positioning (and possibly modifications) of histones, which bind DNA independently of sequence. Conversely, histones and other proteins likely influence ORC binding to DNA, although the relevant mechanisms remain obscure. In this study we used genome-wide location analysis to identify with high accuracy about 500 loci that bind ORC and/or Mcm2p proteins. Within ~70% of these sites we identified DNA sequences that match the consensus for ORC binding, and confirmed that about 80% were required for ARS function. Thus, we have defined the exact position of most ORC binding sites throughout the genome. These findings represents an important contribution that should facilitate future studies of how the interaction between ORC and other chromatin components influences replication origin function, as well as the possibility that ORC regulates chromatin structure or nuclear architecture.

Methods

Genome-wide location analysis

ORC and MCM2 binding sites were identified using genome wide location analysis [24,60]. Target DNA from strain OAy470 was obtained by chromatin immunoprecipitation (ChIP) as described [44]. ORC-bound DNA was isolated from cells arrested with nocodazole (10 μg/mL) for 3 hours at 23°C using anti-ORC polyclonal antibody (1:500) [61]. Mcm2p-bound DNA was isolated from cells arrested in G1 phase with 8.3 ng/mL α-factor (Sigma) for 4 hours at 23°C using anti-Mcm2p antibody (1:50, Santa Cruz). Immunoprecipitated DNA, as well as non-enriched total DNA, was amplified using ligation-mediated-PCR (LM-PCR). Enriched and total DNAs were end-labeled with Cy5 and Cy3, respectively, and co-hybridized to an array designed and synthesized by NimbleGen Systems, Inc. This array contained 124,991 50 bp oligonucleotides tiled every 80 bp across the *S. cerevisiae* genome, present in triplicate. DNA end-labeling, hybridization, and scanning were performed at NimbleGen Systems, Inc., which provided the final text file of foreground signal intensities.

Normalization

The Cy5 and Cy3 foreground signals were converted to log ratio of enrichment defined as $M = \log_2 Cy5 - \log_2 Cy3$ and log intensity defined as $A = (\log_2 Cy5 + \log_2 Cy3)/2$ for each spot. Global loess normalization was applied to remove the systematic effect seen at low intensities on transformed data (see Additional file 13). The normalized M values within the three replicated blocks are highly correlated ($\rho \approx 0.74$) for both ORC and Mcm2p. For each probe, the median of the three replicates was used for further analysis.

HMM-MOG model

A Hidden Markov Model with Mixture of Gaussians (HMM-MOG) was used to fit the data (Figure 1B). The complete parameter set of the model can be described as $\lambda = (\pi, A, B, P)$. Let Q_1 represent the non-enriched state and Q_2 represent the enriched state, $\pi = (\pi_1, \pi_2)$ gives the initial probability of the two states. $A = \{a_{11}\ a_{12}; a_{21}\ a_{22}\}$ denotes the transition probabilities between the two states: a_{ij} is the probability of a transition from state Q_i to state Q_j. $B=\{Y_1, Y_2\}$ is the emission distribution, with $Y_1 \sim N(\mu_1, \sigma_1^2)$ describing M values of non-enriched probes and $Y_2 \sim N(\mu_2, \sigma_2^2)$ describing those of enriched probes. The emission distribution for each state is a mixture of these two Gaussians, but with different mixture proportions described by $P = \{p_{11}, p_{12}; p_{21}\ p_{22}\}$. The idea is essentially to allow a proportion p_{21} of non-enriched probes in an enriched region and a proportion p_{12} of enriched probes in a non-enriched region.

The purpose of including the mixture is to overcome two typical types of error in a ChIP-chip experiment: (1) In non-enriched regions, some probes might behave similar to typical probes in enriched regions, due to possible cross-hybridization; this behavior will cause spikes for a small number of probes. (2) In enriched regions, some probes have weak signals comparable to typical probes in non-enriched regions, due to low hybridization efficiency, non-specificity, etc. These two types of error will occasionally cause improper transitions in a standard HMM (without the mixture) that result in false positive predictions or site breakage. Allowing some amount of false positive probes and some amount of false negative probes makes the HMM more robust to probe failures.

The HMM parameters can be given empirically or estimated from data using the well-known Baum-Welch algorithm for finding the maximum likelihood estimates (MLE) (cf. Rabiner 1989)[62]. To better estimate (π, A, B), we empirically set p_{12}= 6% (false positive probes) and p_{21} = 1% (false negative probes). Experimental tests show that small changes in p_{12} and p_{21} do not change the results significantly. A Viterbi algorithm is used to decode the most probable state sequence to identify unique enriched regions. Because the parameters estimated from the data vary among different chromosomes (see Additional file 1), we standardized all M values to their corresponding Z values to facilitate further comparison.

Peak identification

The Z values were smoothed using a three-probe window over six rounds, which corresponds to a weighted average of 13 probes (~1 kb, which corresponds to the average size of ChIP DNA fragments). The weight distribution is approximately 0.001 : 0.008 : 0.029: 0.069 : 0.123 : 0.173 : 0.193 : 0.173 : 0.123 : 0.069 : 0.029 : 0.008 : 0.001. A

peak is defined by a continuous increase in the smoothed Z value (sZ) for at least five probes followed by a decrease of sZ for another five probes. For each enriched region we report only one peak (with the largest smoothed Z value) every 3 kb. This length was empirically chosen based on analysis of the length of peaks in enriched regions for known ARSs. For long HMM-defined regions (6% of total) multiple peaks were identified. The strength of each peak is defined as the average Z-value (avgZ) for 13 probes, covering ~1 kb. Each HMM region is denoted by the identifying protein(s) and a peak number (e.g. ORC-MCM2-34). If multiple peaks were identified in a region, an additional number is given (e.g. ORC-MCM2-33-1 and ORC-MCM2-33-2).

Motif finding and building an EACS+B1 positional weight matrix

De novo motif finding was carried out separately on ORC-MCM2, ORC-only, and MCM2-only sites using BioProspector with the recommended significance level of p = 2.9 × 10^{-7} (Z value = 5) [63]. A motif length of 17 bp was chosen based on the following prior information: (1) A *de novo* motif finding study on the pro-ARS data set [24] tested a range of motif lengths and showed that 17 bp is the optimum length for retrieving ACSs from the data [22,40]; (2) A previous study also described a 17 bp ACS motif [1,20,21]; (3) The alignment of 31 experimentally verified ACSs shows that these 17 bp are above the 95% quantile (0.17 bits) of the null distribution (estimated from 31 random sequences of 10 kb). Interestingly, the alignment also reveals that the 24th, 31st, 32nd and 33rd positions are significant, where the 32nd and 33rd positions had been previously mapped as B1 element contacted by ORC in ARS1 [38]. Thus we chose to form a two-block motif (named EACS+B1) composed of a 17 bp EACS followed by a 3 bp B1 exactly 13 bp apart (omitting 24th position). A gapped PWM was built on the alignment. We used LOD score to measure the similarity of a test sequence to EACS+B1. Suppose the sequence we are examining is $a_1a_2...a_{33}$. The likelihood of this sequence under the PWM, assuming it is an independent trials model, is

$$P(a_1a_2...a_{33}) = f_{1,a_1} f_{2,a_2} ... f_{17,a_{17}} f_{31,a_{31}} f_{32,a_{32}} f_{33,a_{33}},$$

where f_{i,a_i} is the probability of observing base a_i in position i in the PWM. The corresponding probability under the background model is

$$P(a_1a_2...a_{33}) = q_{a_1} q_{a_2} ... q_{a_{17}} q_{a_{31}} q_{a_{32}} q_{a_{33}},$$

where q_{a_i} is the genomic frequency of base a_i. The log-likelihood is defined as

$$LOD = \sum_{i=1,2...17,31,32,33} \log \frac{f_{i,a_i}}{q_{a_i}}.$$

The LOD score was converted to a p-value based on the null distribution generated by scanning EACS+B1 throughout chromosome VI, excluding all identified ARSs. Sensitivity was obtained by a three-fold cross-validation. Briefly, the 31 ACSs were divided randomly into subgroups of 10, 10, and 11 ACSs, and each subgroup was scored by the PWM with parameters estimated from the other two subgroups. The number of ACSs with scores above a chosen threshold divided by 31 indicates the sensitivity.

The inter motif similarity between motif A and B is defined as

$$S(A,B) = 1 - \frac{1}{2W} \sum_{i=1}^{W} \sum_{j=1}^{4} \left| f_{i,j}^{A} - f_{i,j}^{B} \right|,$$

where W is the motif length, $f_{i,j}^{A}$ and $f_{i,j}^{B}$ are the observed frequency of base j at position i in motif A and B respectively. The similarity is between 0 and 1; multiplying by 100 gives the similarity as a percentage.

Determination of ARS and ACS function

ARS activity was determined by testing the ability of a sequence of interest to confer replication to a plasmid otherwise lacking a functional yeast ARS as described by Wyrick et al. [24], or by a co-transformation approach that takes advantage of yeast's high frequency of homologous recombination. For the latter method, the sequence of interest was amplified from yeast genomic DNA using primers that each contains 20 bp of homology to the sequence of interest and 40 bp of homology to either end of a gapped *CEN4/URA3* vector lacking an ARS. The amplified product was co-transformed into yeast (*ura3-1*) with the gapped vector, and transformants were selected on -URA. A high frequency of transformation depended on the presence of an ARS sequence in the amplified DNA, while colony size reflected the efficiency of ARS function. For classification, ARS305 was used as the standard for normal ARS function and ARS604 as representative of a weak ARS. Weak ARSs exhibit a high frequency of transformation, but form smaller colonies than cells harboring ARS305, requiring about three days, rather than two, to form a colony ~3 mm in diameter. Very weak ARSs also showed a high frequency of transformation, but colonies were small after three days and grew slowly upon restreaking. These assays were performed in duplicate.

To test the requirement of potential ACSs for ARS function, PCR primers were designed to amplify the ARS

region in two fragments each of which has an endpoint in the 11 bp ACS. The ACS was replaced with a restriction site to allow ligation of the two fragments. The distal ends of these two fragments also contained introduced restriction sites for ligation into a vector lacking yeast ARS function. If deletion of an ACS resulted in loss of the high transformation frequency of the ARS, the ACS was denoted as functional.

Data deposition

Data from this work is being submitted to the *Saccharomyces* Genome Database. Data will also be available at the DNA Replication Origin Database [64], which includes a graphic viewer format of the nimARS data similar to that of Figure 7B.

Authors' contributions

WX performed computational analyses. JGA performed experimental work. All authors contributed to the conception and experimental design, and to manuscript drafts and revisions.

Additional material

Additional file 1

HMM parameters. See Methods for explanation.

Click here for file

[http://www.biomedcentral.com/content/supplementary/1471-2164-7-276-S1.xls]

Additional file 2

ORC-only sites.

Click here for file

[http://www.biomedcentral.com/content/supplementary/1471-2164-7-276-S2.xls]

Additional file 3

MCM2-only sites.

Click here for file

[http://www.biomedcentral.com/content/supplementary/1471-2164-7-276-S3.xls]

Additional file 4

ORC-MCM2 sites.

Click here for file

[http://www.biomedcentral.com/content/supplementary/1471-2164-7-276-S4.xls]

Additional file 5

Identification of known ARS.

Click here for file

[http://www.biomedcentral.com/content/supplementary/1471-2164-7-276-S5.xls]

Additional file 12

Logo of 31 known ACSs demonstrates the EACS+B1 element. The dashed line shows 95% quantile (0.17 bits) of information content distribution of 31 10,000 bp random sequences. Based on the cutoff, we used a 17 bp EACS + 3 bp B1 to construct a gapped PWM to scan nimARS.

Click here for file

[http://www.biomedcentral.com/content/supplementary/1471-2164-7-276-S12.pdf]

Additional file 6

Set of nimARS.

Click here for file

[http://www.biomedcentral.com/content/supplementary/1471-2164-7-276-S6.xls]

Additional file 10

Verified nimARS. Coordinates of regions tested for ARS activity are provided. ARS names are assigned to be consistent with Wyrick et al. [24] and the DNA replication origin database [64].

Click here for file

[http://www.biomedcentral.com/content/supplementary/1471-2164-7-276-S10.xls]

Additional file 11

False predictions of Wyrick et al. [24].

Click here for file

[http://www.biomedcentral.com/content/supplementary/1471-2164-7-276-S11.xls]

Additional file 7

Known ACS.

Click here for file

[http://www.biomedcentral.com/content/supplementary/1471-2164-7-276-S7.xls]

Additional file 8

Predicted nimACS.

Click here for file

[http://www.biomedcentral.com/content/supplementary/1471-2164-7-276-S8.xls]

Additional file 9

Verified nimACS.

Click here for file

[http://www.biomedcentral.com/content/supplementary/1471-2164-7-276-S9.doc]

Additional file 13

Normalization using global loess. The red line indicates the loess line. M is the log of ratio of IP divided by total (also termed enrichment score) and A is the average log intensity.

Click here for file

[http://www.biomedcentral.com/content/supplementary/1471-2164-7-276-S13.pdf]

Acknowledgements

We thank Y. Chowdhury, R. Nam, and Z. Shen for excellent technical assistance, and Steve Bell for anti-ORC antibody. This work was supported by NIH grants R01GM67243 (to ST) and RO1GM65494 (to OMA) and grant IRG-58-007-42 from the American Cancer Society (to OMA).

References

1. Bell SP: **The origin recognition complex: from simple origins to complex functions.** *Genes Dev* 2002, **16(6):**659-672.
2. DePamphilis ML: **The 'ORC cycle': a novel pathway for regulating eukaryotic DNA replication.** *Gene* 2003, **310:**1-15.
3. Bell SP, Dutta A: **DNA replication in eukaryotic cells.** *Annu Rev Biochem* 2002, **71:**333-374.
4. Machida YJ, Hamlin JL, Dutta A: **Right place, right time, and only once: replication initiation in metazoans.** *Cell* 2005, **123(1):**13-24.
5. Lipford JR, Bell SP: **Nucleosomes positioned by ORC facilitate the initiation of DNA replication.** *Mol Cell* 2001, **7(1):**21-30.
6. Aparicio JG, Viggiani CJ, Gibson DG, Aparicio OM: **The Rpd3-Sin3 histone deacetylase regulates replication timing and enables intra-S origin control in Saccharomyces cerevisiae.** *Mol Cell Biol* 2004, **24(11):**4769-4780.
7. Vogelauer M, Rubbi L, Lucas I, Brewer BJ, Grunstein M: **Histone acetylation regulates the time of replication origin firing.** *Mol Cell* 2002, **10(5):**1223-1233.
8. Aggarwal BD, Calvi BR: **Chromatin regulates origin activity in Drosophila follicle cells.** *Nature* 2004, **430(6997):**372-376.
9. Weinreich M, Palacios DeBeer MA, Fox CA: **The activities of eukaryotic replication origins in chromatin.** *Biochim Biophys Acta* 2004, **1677(1–3):**142-157.
10. Muller M, Lucchini R, Sogo JM: **Replication of yeast rDNA initiates downstream of transcriptionally active genes.** *Mol Cell* 2000, **5(5):**767-777.
11. Marahrens Y, Stillman B: **A yeast chromosomal origin of DNA replication defined by multiple functional elements.** *Science* 1992, **255(5046):**817-823.
12. Lemaitre JM, Danis E, Pasero P, Vassetzky Y, Mechali M: **Mitotic remodeling of the replicon and chromosome structure.** *Cell* 2005, **123(5):**787-801.
13. Cvetic C, Walter JC: **Eukaryotic origins of DNA replication: could you please be more specific?** *Semin Cell Dev Biol* 2005, **16(3):**343-353.
14. Kohzaki H, Murakami Y: **Transcription factors and DNA replication origin selection.** *Bioessays* 2005, **27(11):**1107-1116.
15. Gilbert DM: **Making sense of eukaryotic DNA replication origins.** *Science* 2001, **294(5540):**96-100.
16. Norio P, Kosiyatrakul S, Yang Q, Guan Z, Brown NM, Thomas S, Riblet R, Schildkraut CL: **Progressive activation of DNA replication initiation in large domains of the immunoglobulin heavy chain locus during B cell development.** *Mol Cell* 2005, **20(4):**575-587.
17. Mesner LD, Hamlin JL: **Specific signals at the 3' end of the DHFR gene define one boundary of the downstream origin of replication.** *Genes Dev* 2005, **19(9):**1053-1066.
18. Sasaki T, Ramanathan S, Okuno Y, Kumagai C, Shaikh SS, Gilbert DM: **The Chinese hamster dihydrofolate reductase replication origin decision point follows activation of transcription and suppresses initiation of replication within transcription units.** *Mol Cell Biol* 2006, **26(3):**1051-1062.
19. MacAlpine DM, Rodriguez HK, Bell SP: **Coordination of replication and transcription along a Drosophila chromosome.** *Genes Dev* 2004, **18(24):**3094-3105.
20. Newlon CS, Theis JF: **The structure and function of yeast ARS elements.** *Curr Opin Genet Dev* 1993, **3(5):**752-758.
21. Theis JF, Newlon CS: **The ARS309 chromosomal replicator of Saccharomyces cerevisiae depends on an exceptional ARS consensus sequence.** *Proc Natl Acad Sci USA* 1997, **94(20):**10786-10791.
22. Breier AM, Chatterji S, Cozzarelli NR: **Prediction of Saccharomyces cerevisiae replication origins.** *Genome Biol* 2004, **5(4):**R22.
23. Natale DA, Umek RM, Kowalski D: **Ease of DNA unwinding is a conserved property of yeast replication origins.** *Nucleic Acids Res* 1993, **21(3):**555-560.
24. Wyrick JJ, Aparicio JG, Chen T, Barnett JD, Jennings EG, Young RA, Bell SP, Aparicio OM: **Genome-wide distribution of ORC and MCM proteins in S. cerevisiae: high-resolution mapping of replication origins.** *Science* 2001, **294(5550):**2357-2360.
25. Snyder M, Sapolsky RJ, Davis RW: **Transcription interferes with elements important for chromosome maintenance in Saccharomyces cerevisiae.** *Mol Cell Biol* 1988, **8(5):**2184-2194.
26. Nieduszynski CA, Blow JJ, Donaldson AD: **The requirement of yeast replication origins for pre-replication complex proteins is modulated by transcription.** *Nucleic Acids Res* 2005, **33(8):**2410-2420.
27. Miyake T, Loch CM, Li R: **Identification of a multifunctional domain in autonomously replicating sequence-binding factor 1 required for transcriptional activation, DNA replication, and gene silencing.** *Mol Cell Biol* 2002, **22(2):**505-516.
28. Simpson RT: **Nucleosome positioning can affect the function of a cis-acting DNA element in vivo.** *Nature* 1990, **343(6256):**387-389.
29. Venditti P, Costanzo G, Negri R, Camilloni G: **ABF1 contributes to the chromatin organization of Saccharomyces cerevisiae ARS1 B-domain.** *Biochim Biophys Acta* 1994, **1219(3):**677-689.
30. MacAlpine DM, Bell SP: **A genomic view of eukaryotic DNA replication.** *Chromosome Res* 2005, **13(3):**309-326.
31. Jeon Y, Bekiranov S, Karnani N, Kapranov P, Ghosh S, MacAlpine D, Lee C, Hwang DS, Gingeras TR, Dutta A: **Temporal profile of replication of human chromosomes.** *Proc Natl Acad Sci USA* 2005, **102(18):**6419-6424.
32. Raghuraman MK, Winzeler EA, Collingwood D, Hunt S, Wodicka L, Conway A, Lockhart DJ, Davis RW, Brewer BJ, Fangman WL: **Replication dynamics of the yeast genome.** *Science* 2001, **294(5540):**115-121.
33. Yabuki N, Terashima H, Kitada K: **Mapping of early firing origins on a replication profile of budding yeast.** *Genes Cells* 2002, **7(8):**781-789.
34. Feng W, Collingwood D, Boeck ME, Fox LA, Alvino GM, Fangman WL, Raghuraman MK, Brewer BJ: **Genomic mapping of single-stranded DNA in hydroxyurea-challenged yeasts identifies origins of replication.** *Nat Cell Biol* 2006, **8(2):**148-155.
35. Poloumienko A, Dershowitz A, De J, Newlon CS: **Completion of replication map of Saccharomyces cerevisiae chromosome III.** *Mol Biol Cell* 2001, **12(11):**3317-3327.
36. Shirahige K, Iwasaki T, Rashid MB, Ogasawara N, Yoshikawa H: **Location and characterization of autonomously replicating sequences from chromosome VI of Saccharomyces cerevisiae.** *Mol Cell Biol* 1993, **13(8):**5043-5056.
37. Friedman KL, Brewer BJ, Fangman WL: **Replication profile of Saccharomyces cerevisiae chromosome VI.** *Genes Cells* 1997, **2(11):**667-678.
38. Lee DG, Bell SP: **Architecture of the yeast origin recognition complex bound to origins of DNA replication.** *Mol Cell Biol* 1997, **17(12):**7159-7168.
39. Bulyk ML, McGuire AM, Masuda N, Church GM: **A motif co-occurrence approach for genome-wide prediction of transcription-factor-binding sites in Escherichia coli.** *Genome Res* 2004, **14(2):**201-208.
40. Xu W: **Searching for and beyond yeast replication origins.** Los Angeles: University of Southern California; 2006.
41. Xing EP, Wu W, Jordan MI, Karp RM: **LOGOS: a modular Bayesian model for de novo motif detection.** *Proc IEEE Comput Soc Bioinform Conf* 2003, **2:**266-276.
42. Wu J: **Statistical Inference for Molecular Data: Man, Motifs, and Microarrays.** Los Angeles: University of Southern California; 2001.
43. Nieduszynski CA, Knox Y, Donaldson AD: **Genome-wide identification of replication origins in yeast by comparative genomics.** *Genes Dev* 2006, **20(14):**1874-1879.
44. Aparicio OM, Weinstein DM, Bell SP: **Components and dynamics of DNA replication complexes in S. cerevisiae: redistribution of MCM proteins and Cdc45p during S phase.** *Cell* 1997, **91(1):**59-69.
45. Harvey KJ, Newport J: **Metazoan origin selection: origin recognition complex chromatin binding is regulated by CDC6 recruitment and ATP hydrolysis.** *J Biol Chem* 2003, **278(49):**48524-48528.
46. Mizushima T, Takahashi N, Stillman B: **Cdc6p modulates the structure and DNA binding activity of the origin recognition complex in vitro.** *Genes Dev* 2000, **14(13):**1631-1641.

47. Fletcher RJ, Bishop BE, Leon RP, Sclafani RA, Ogata CM, Chen XS: **The structure and function of MCM from archaeal M. Thermoautotrophicum.** *Nat Struct Biol* 2003, **10(3):**160-167.
48. Pape T, Meka H, Chen S, Vicentini G, van Heel M, Onesti S: **Hexameric ring structure of the full-length archaeal MCM protein complex.** *EMBO Rep* 2003, **4(11):**1079-1083.
49. Bowers JL, Randell JC, Chen S, Bell SP: **ATP hydrolysis by ORC catalyzes reiterative Mcm2-7 assembly at a defined origin of replication.** *Mol Cell* 2004, **16(6):**967-978.
50. Donovan S, Harwood J, Drury LS, Diffley JF: **Cdc6p-dependent loading of Mcm proteins onto pre-replicative chromatin in budding yeast.** *Proc Natl Acad Sci USA* 1997, **94(11):**5611-5616.
51. Rowles A, Tada S, Blow JJ: **Changes in association of the Xenopus origin recognition complex with chromatin on licensing of replication origins.** *J Cell Sci* 1999, **112(Pt 12):**2011-2018.
52. Hua XH, Newport J: **Identification of a preinitiation step in DNA replication that is independent of origin recognition complex and cdc6, but dependent on cdk2.** *J Cell Biol* 1998, **140(2):**271-281.
53. Vujcic M, Miller CA, Kowalski D: **Activation of silent replication origins at autonomously replicating sequence elements near the HML locus in budding yeast.** *Mol Cell Biol* 1999, **19(9):**6098-6109.
54. Santocanale C, Sharma K, Diffley JF: **Activation of dormant origins of DNA replication in budding yeast.** *Genes Dev* 1999, **13(18):**2360-2364.
55. Dubey DD, Davis LR, Greenfeder SA, Ong LY, Zhu JG, Broach JR, Newlon CS, Huberman JA: **Evidence suggesting that the ARS elements associated with silencers of the yeast mating-type locus HML do not function as chromosomal DNA replication origins.** *Mol Cell Biol* 1991, **11(10):**5346-5355.
56. Ak P, Benham CJ: **Susceptibility to superhelically driven DNA duplex destabilization: a highly conserved property of yeast replication origins.** *PLoS Comput Biol* 2005, **1(1):**e7.
57. McConnell KH, Muller P, Fox CA: **Tolerance of Sir1p/origin recognition complex-dependent silencing for enhanced origin firing at HMRa.** *Mol Cell Biol* 2006, **26(5):**1955-1966.
58. Irlbacher H, Franke J, Manke T, Vingron M, Ehrenhofer-Murray AE: **Control of replication initiation and heterochromatin formation in Saccharomyces cerevisiae by a regulator of meiotic gene expression.** *Genes Dev* 2005, **19(15):**1811-1822.
59. Dershowitz A, Newlon CS: **The effect on chromosome stability of deleting replication origins.** *Mol Cell Biol* 1993, **13(1):**391-398.
60. Ren B, Robert F, Wyrick JJ, Aparicio O, Jennings EG, Simon I, Zeitlinger J, Schreiber J, Hannett N, Kanin E, *et al.*: **Genome-wide location and function of DNA binding proteins.** *Science* 2000, **290(5500):**2306-2309.
61. Klemm RD, Bell SP: **ATP bound to the origin recognition complex is important for preRC formation.** *Proc Natl Acad Sci USA* 2001, **98(15):**8361-8367.
62. Rabiner L: **A tutorial on hidden Markov models and selected apllications in speech recognition.** *Proceedings of the IEEE* 1989, **77:**257-286.
63. Liu X, Brutlag DL, Liu JS: **BioProspector: discovering conserved DNA motifs in upstream regulatory regions of co-expressed genes.** *Pac Symp Biocomput* 2001:127-138.
64. **DNA Replication Origin Database** [http://www.oridb.org]
65. **WebLogo** [http://weblogo.berkeley.edu]